

Supplementary Information:

Spatially controlled epitaxial growth of 2D heterostructures via defect-engineering using a focused He ion beam

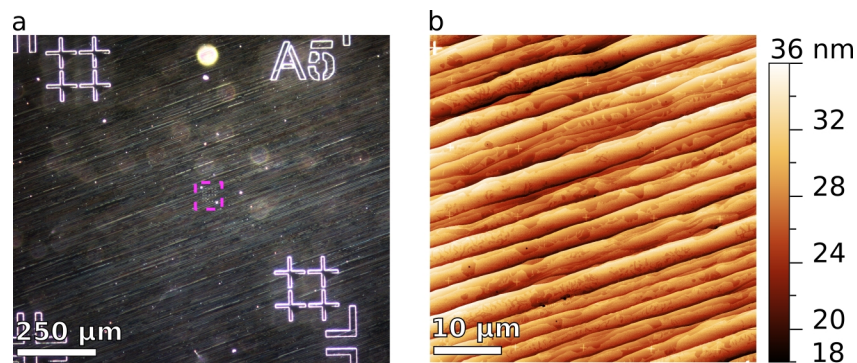
Martin Heilmann¹, Victor Deinhart^{2,3}, Abbas Tahraoui¹, Katja Höflich³, and J. Marcelo J. Lopes¹

¹Paul-Drude-Institut für Festkörperelektronik, Leibniz-Institut im Forschungsverbund Berlin e.V.,
Hausvogteiplatz 5-7, 10117 Berlin, Germany

²Ferdinand-Braun Institut, Leibniz-Institut für Höchstfrequenztechnik, Gustav-Kirchhoff-Str. 4,
12489 Berlin, Germany

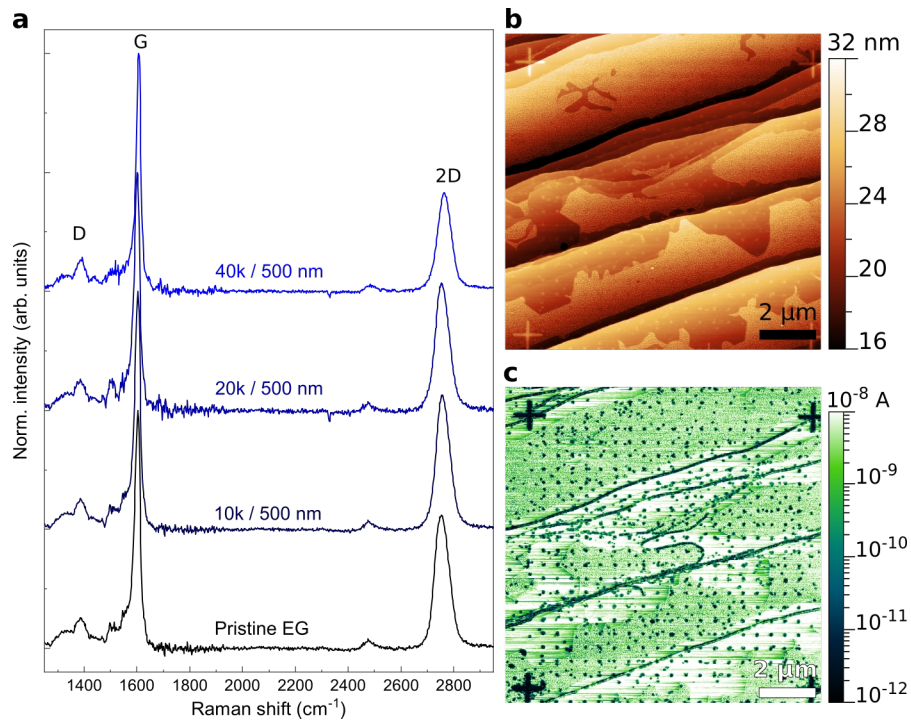
³Helmholtz-Zentrum Berlin für Materialien und Energie GmbH, Hahn-Meitner-Platz 1, 14109
Berlin, Germany

For locating the areas structured with a He focused ion beam (FIB) the 10x10 mm² SiC samples were first structured with markers via photolithography and reactive ion etching using SF₆. After the processing of epitaxial graphene (EG) the markers were still visible (see dark field micrograph in Supplementary Figure 1a and the FIB pattern (marked by the magenta framed square, and as shown in Figure 1d in the main text) was aligned to them. Supplementary Figure 1b shows the morphology of one structured area after the growth of h-BN for 300 min, as measured by atomic force microscopy (AFM). On the terraces rougher areas can be distinguished from smoother areas close to the step edges, which we attribute to overgrown single- (SLG) and bi-layer graphene (BLG). Previous studies already demonstrated faster growth rates of disordered h-BN on SLG due to an atomic corrugation of the SLG, induced by the closer proximity to the interface layer to SiC, which is screened by an additional graphene layer in BLG.¹



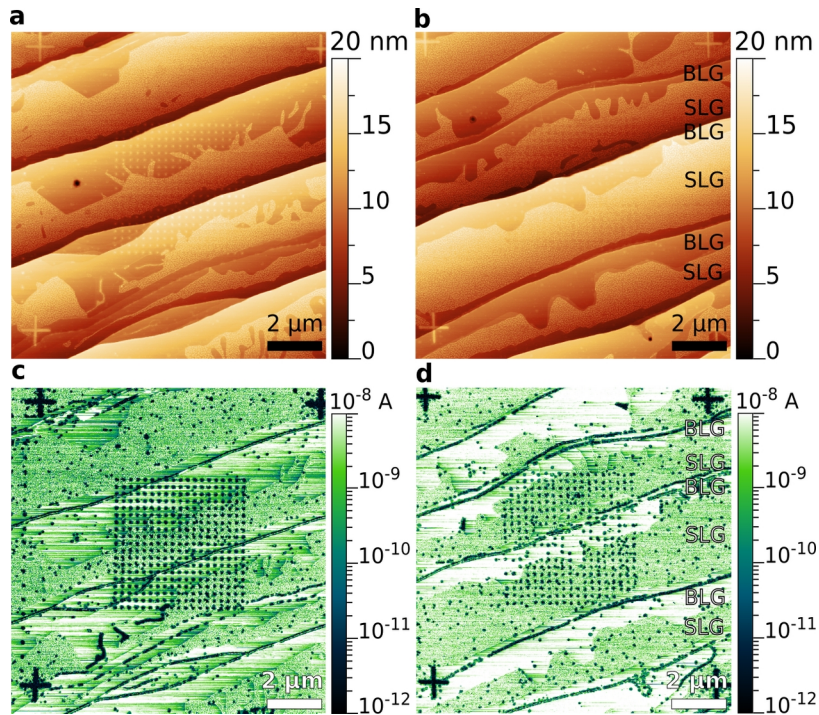
Supplementary Figure 1. a) Dark-field micrograph of a marker on the substrate with the FIB pattern marked by the magenta dotted square. b) AFM image of the patterned area.

Supplementary Figure 2 compares the mean Raman spectra for the FIB pattern with 500 nm distance between the irradiation induced defects (IIDs) written with varying numbers of He ions. Unlike in pattern with a distance of 250 nm between the IIDs shown in Figure 1 of the main text, only in the case of 40000 ions per IID a slight increase in the D peak intensity was observed, due to the lower density of defects in this pattern. The AFM image in Supplementary Figure 2b shows a sample area with IIDs written with 20000 ions per defect after the growth for 300 minutes at 850 °C. The corresponding conductive AFM (cAFM) image shown in Supplementary Figure 2c shows the position of the h-BN islands within the marked area.



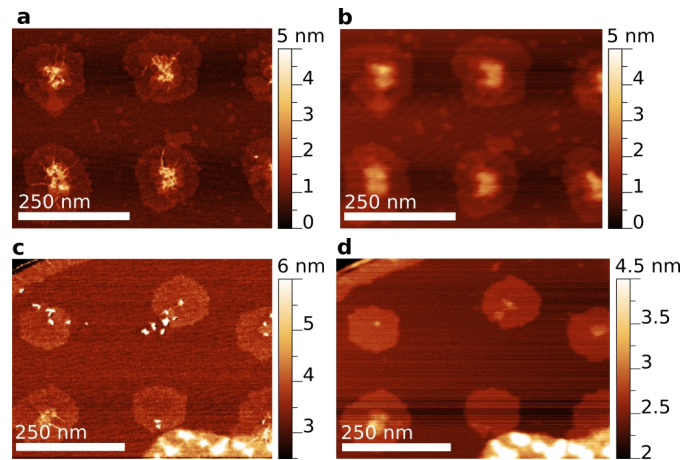
Supplementary Figure 2. a) Comparison of the mean Raman spectra of patterns with 500 nm distance between the IIDs density written with varying number of He ions per defect. The spectra were normalized with respect to the G peak and vertically shifted for clarity. b) AFM images of an area with 19x19 defects written with 20 000 ions per IID in a distance of 500 nm to each other between the cross-shaped markers, with the (c) corresponding cAFM image at a bias of 100 mV applied to graphene showing the position of the insulating h-BN islands.

Supplementary Figure 3 shows the morphology and cAFM images of areas structured with 40000 (Supplementary Figure 3a,c) and 10000 (Supplementary Figure 3b,d) He ions per defect location after the growth of h-BN for 300 min. A difference in nucleation yield is apparent, where for fewer He ions only 86 % of the IIDs on the terraces resulted in a nucleation of h-BN. In the AFM image shown in Supplementary Figure 3b also the single-layer (SLG) and bi-layer graphene (BLG) areas are marked, demonstrating a different roughness as discussed earlier¹.



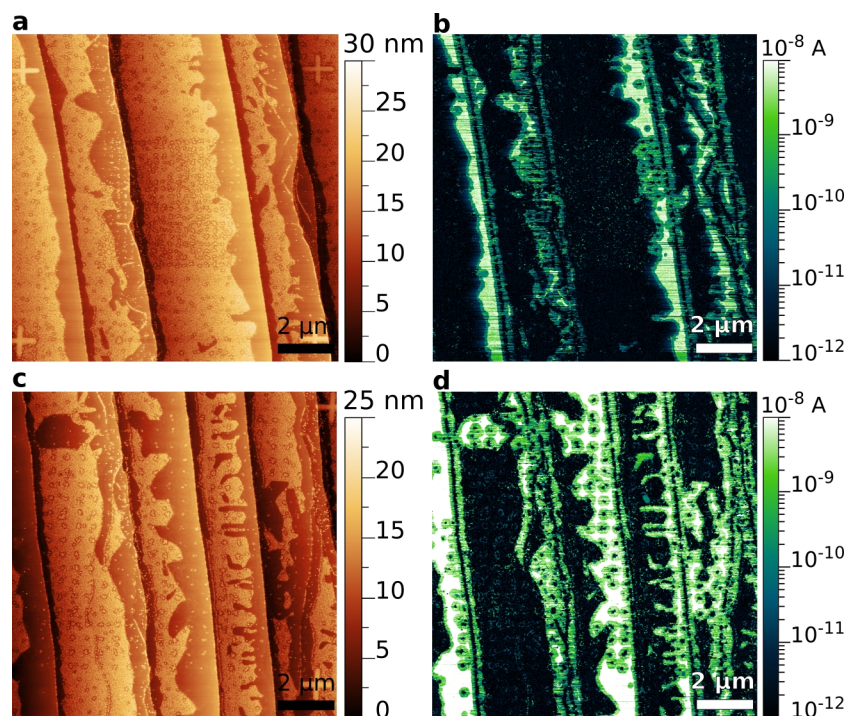
Supplementary Figure 3. AFM images of patterned areas with (a) 40000 and (b) 10000 ions per IID after the growth of h-BN for 300 min, with the cAFM images in (c) and (d), respectively. In (b) and (c) the SLG and BLG areas are marked.

Due to the imaging in contact mode during cAFM measurements, some nanoparticles (NPs) were removed from the epitaxially aligned h-BN islands nucleating at IIDs written with 10000 He ions each, as shown in Supplementary Figure 4 for a comparison before (a,c) and after (b,d) the cAFM scan.



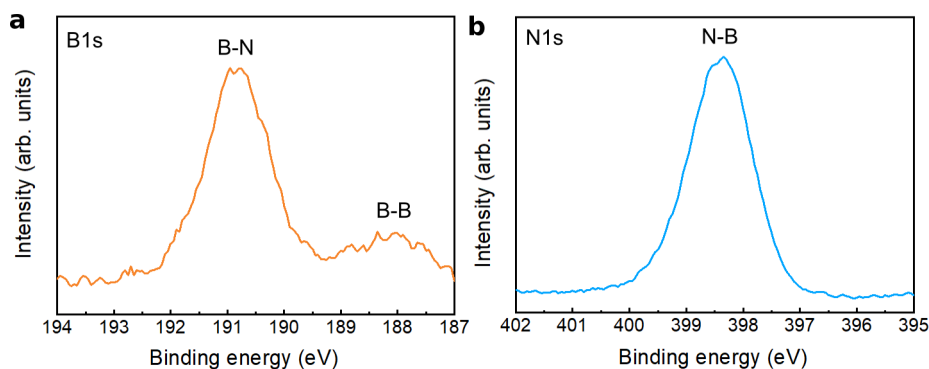
Supplementary Figure 4. AFM images of h-BN islands in patterned areas with 40000 ions per IID (a) before and (b) after cAFM measurements, show no change in morphology. AFM image of h-BN islands nucleating at IIDs written with 10000 He ions (c) before and (d) after cAFM measurements show the removal of some NPs.

Supplementary Figure 5a shows an AFM image of the surface of a patterned area with 20000 He ions per IID (with a distance of 250 nm to each other) after the overgrowth of h-BN for 480 min with increased B deposition rate, with the corresponding cAFM image shown in Supplementary Figure 5b. Due to their atomic corrugation the SLG areas are completely overgrown with multiple, disordered h-BN layers¹ and appear mostly insulating. On BLG only in the patterned area one completely coalesced h-BN layer formed, while in the non-patterned BLG areas h-BN is mostly growing at step edges and wrinkles, leaving large parts of graphene uncovered. Supplementary Figure 5c shows an AFM image of the same sample, with the IIDs in a distance of 500 nm after the overgrowth with h-BN, with the corresponding cAFM image in (d). On BLG separated islands with a mean diameter of 450 nm are apparent. Considering their nucleation at the IIDs in the center of the islands the higher deposition rate resulted in a lateral growth rate of nearly 0.47 nm/min, which is considerably faster than the 0.25 nm/min when using the lower B deposition rate (see Figure 2 in the main text).



Supplementary Figure 5. a) AFM image of patterned areas with IIDs in a distance of 250 nm, after the growth of h-BN for 480 min at increased B deposition rate, with the corresponding cAFM image in (b), demonstrating a coalesced h-BN layer between the IIDs. c) AFM image of the same sample, in an area with a distance of 500 nm between the IIDs with the corresponding cAFM image in (d), demonstrating the formation of individual h-BN islands at the IIDs on BLG.

To study the chemical bonds in the sample with higher boron deposition rate and increased growth time (see Figure 4 in the main manuscript and Supplementary Figure 5) XPS measurements were performed in the B1s and N1s spectral regions (see Methods section in the main manuscript). The dominant peak in the B1s spectral region (Supplementary Figure 6a) at 190.8 eV is attributed to B bonded to N and the peak at 398.4 eV in the N1s spectral region (Supplementary Figure 6b) is attributed to N bonded to B. These values are in good agreement with previously recorded values for MBE grown h-BN on EG² and graphite³. A small peak in the B1s spectral region at ~ 188 eV is indicative of B-B bonds⁴. This peak is attributed to B clustering at the cross-shaped marker structures (as visible in the corners of the AFM image in Supplementary Figure 5a).

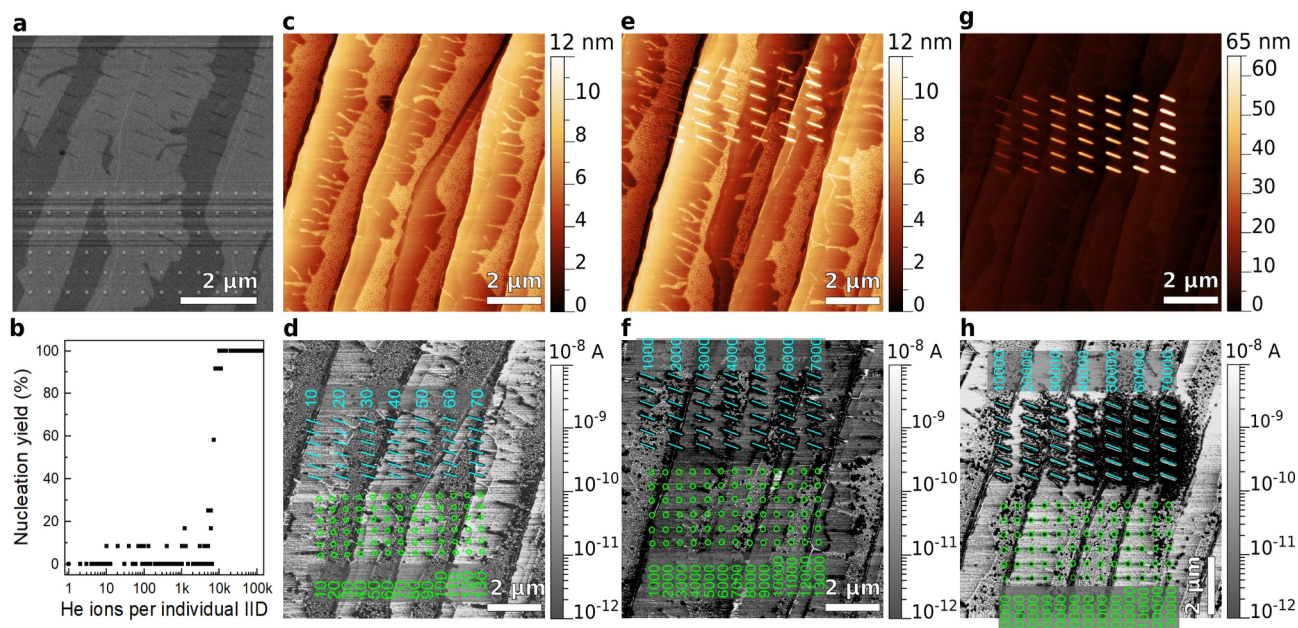


Supplementary Figure 6. a) B1s and (b) N1s core level spectra of h-BN grown on EG for 480 min at elevated B flow rates.

The appropriate ion number for creating defects which initiate nucleation was determined on test samples, where the number of ions was varied over several orders of magnitude covering the range from one ion per IID up to 130000 ions. A typical test pattern for this purpose contained 6 individual IIDs (in a distance of 500 nm) as well as overlapping IIDs written along 6 lines, each 500 nm long. The SEM image shown in Supplementary Figure 7a shows a patterned area, where the highest numbers of ions were used. The dark and bright contrast in the sample are attributed to SLG and BLG. The individual IIDs are visible with a relatively higher contrast, while the IIDs written along lines appear darker as the background. To study the nucleation yield, the test structures were loaded into the MBE and h-BN was grown for 300 minutes at 850 °C with the same sources and settings as described in the main text. Two repetitions of these structures were then analyzed using AFM and cAFM. Supplementary Figure 7b summarizes the results for the individual IIDs, where below ~ 1000 ions per IID no preferential nucleation could be observed at the defects. Only in few cases here an island probably grew at a location of an IID by chance (see AFM image in Supplementary Figure 7c with corresponding cAFM image in Supplementary Figure 7d). Above 10000 He ions in each location of an IID an insulating h-BN island could be found leading to the nucleation yield of 100 % (see AFM image in Supplementary Figure 7e and 7g with corresponding cAFM image in Supplementary Figure 7f and 7h, respectively). The difference to the nucleation yield of 86 % at 10000 He ions per IID observed in the structures shown in the main text is attributed to the lower amount of IIDs written in the test structures.

The intention behind the overlapping IIDs written along lines was to use them as markers to locate the patterned areas after the growth. Here we decided to use 70000 ions per IID, where after the growth lines with a height above 50 nm could be observed (see Supplementary Figure 7g). In between the patterned areas additional cross-shaped markers were written (e.g. as shown in

Supplementary Figure 3) using 2000 ions per overlapping IID. After the growth the height of these cross-shaped markers amounted to ~ 2 nm.



Supplementary Figure 7. a) SEM image of a typical test pattern where in each of the 13 rows, 6 individual IIDs were written 500 nm below each other using between 10000 and 130000 ions per IID. The 7 rows with overlapping IIDs written along lines visible above were written with 10000 to 70000 He ions per IID. b) Nucleation yield for h-BN grown for 300 minutes on the individual IIDs. c-h) Exemplary test structures written with varying number of ions after the growth of h-BN. c) AFM image of test structure written with 10 to 130 ions per individual IID (positions marked by green colored circles) and 10 to 70 ions per overlapping IID (position marked by cyan colored lines). The locations of the IIDs and the number of He ions used per IID in the different rows are noted in the corresponding cAFM image in (d). e) AFM image and (f) corresponding cAFM image of test structure where between 1000 and 13000 He ions were used per individual IID and between 1000 and 7000 He ions per overlapping IID. g) AFM image and (h) corresponding cAFM image of test structure where between 10000 and 130000 He ions were used per individual IID and between 10000 and 70000 He ions per overlapping IID.

Supplementary References

1. Heilmann, M. *et al.* Influence of Proximity to Supporting Substrate on van der Waals Epitaxy of Atomically Thin Graphene/Hexagonal Boron Nitride Heterostructures. *ACS Appl. Mater. Interfaces* **12**, 8897–8907 (2020).
2. Heilmann, M., Bashouti, M., Riechert, H. & Lopes, J. M. J. Defect mediated van der Waals epitaxy of hexagonal boron nitride on graphene. *2D Mater.* **5**, (2018).
3. Cho, Y. *et al.* Hexagonal Boron Nitride Tunnel Barriers Grown on Graphite by High Temperature Molecular Beam Epitaxy. *Sci. Rep.* **6**, 34474 (2016).
4. Bresnehan, M. S. *et al.* Prospects of direct growth boron nitride films as substrates for graphene electronics. *J. Mater. Res.* **29**, 459–471 (2014).